Eikonal method for Borromean nuclei

E. C. Pinilla, P. Descouvemont and D. Baye

Université Libre de Bruxelles, Brussels, Belgium

Outline

1. Motivation

2. Introduction

3. Four-body eikonal method

4. Three-body projectile
   - Bound states
   - Scattering states

5. Applications
   - ^{6}He
   - ^{11}Li

6. Conclusions

Motivation

To study elastic scattering and breakup cross sections of ^{11}Li in a four-body eikonal model.

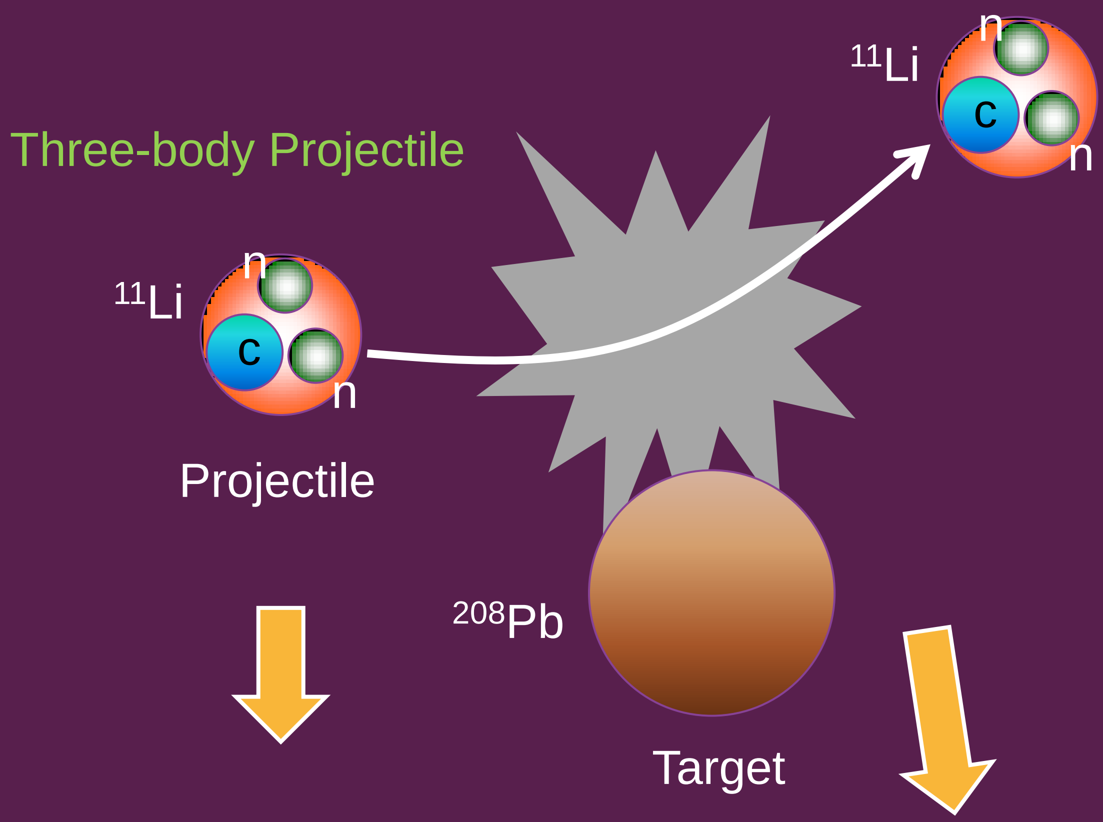

- Bound states
- Continuum states
- Dipole strengths

- Four-body elastic scattering cross sections

Motivation

To study elastic scattering and breakup cross sections of ^{11}Li in a four-body eikonal model.

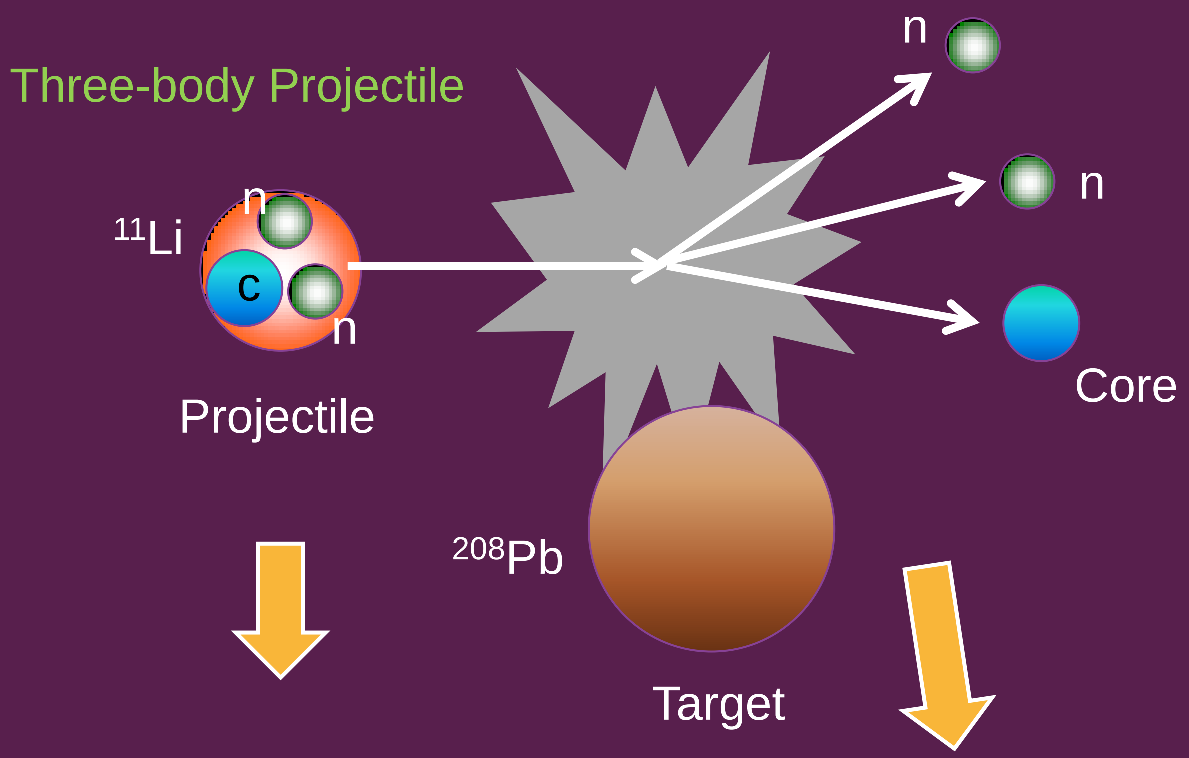

- Bound states
- Continuum states
- Dipole strengths

- Breakup cross sections
- Angular distributions

Introduction

- High-energy reactions are widely used to investigate Halo nuclei.
- High incident energies permits to handle the Schrödinger equation in a simplified way: Eikonal method.
- Non-microscopic 2-Body and 3-Body descriptions of the projectile has been introduced in the eikonal method.

Two-body projectile

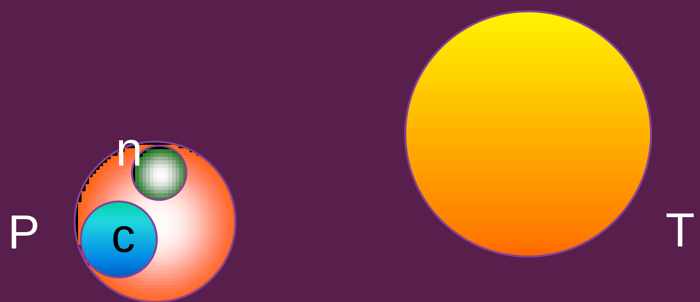

Elastic scattering, breakup
Ex: $^{11}Be+^{208}Pb=(^{10}Be+n)+^{208}Pb$
G. Goldstein, et. al; Phys. Rev. C 73, 024602 (2006).

Three-body projectile

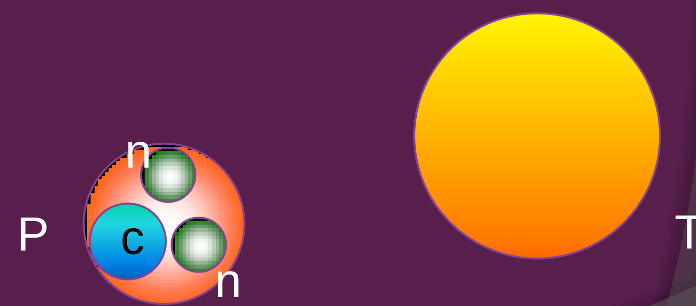

Elastic scattering, breakup
Ex: $^{6}He+^{208}Pb=(\alpha+n+n)+^{208}Pb$
D. Baye, et. al; Phys. Rev. C 79, 024607 (2009).

Eikonal approximation for one-body projectile

We have to solve the Schrödinger equation

$$\left[-\frac{\hbar^2}{2\mu_{PT}}\Delta + V_{PT}(r)\right]\Phi(\boldsymbol{r}) = E\Phi(\boldsymbol{r}).$$

At high-energies the wave function: Smooth deviation from a plane wave

$$\Phi(\boldsymbol{r}) = \frac{1}{(2\pi)^{3/2}} e^{iKZ}\,\widehat{\Phi}(\boldsymbol{r}),$$

Smoothly varying function

we have

$$-\frac{\hbar^2}{2\mu_{PT}}\left[\Delta + 2iK\frac{\partial}{\partial Z} + V_{PT}(r)\right]\widehat{\Phi}(\boldsymbol{r}) = 0.$$

At high-energies $\left|\Delta\widehat{\Phi}\right| \ll K\left|\frac{\partial\widehat{\Phi}}{\partial Z}\right|$, then

$$\Phi^{\text{eik}} = \frac{1}{(2\pi)^{3/2}}\exp[iKZ - \frac{i}{\hbar v}\int_{-\infty}^{Z} V_{PT}(\boldsymbol{b}, Z')dZ'].$$

Structureless projectile

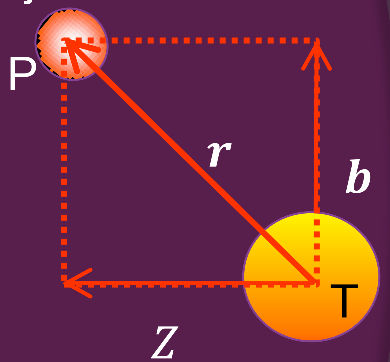

Structureless Target

Eikonal approximation for one body projectile

Ex: Elastic scattering of an incident uncharged particle

The elastic amplitude

$$f(\theta) = iK\int_0^\infty J_0(qb)\left[1 - e^{i\chi(b)}\right]bdb; \quad q = 2K\sin\frac{\theta}{2}$$

The eikonal phase

$$\chi(b) = -\frac{1}{\hbar\, v}\int_{-\infty}^{\infty} V_{PT}(b,Z)dZ; \;\; v = \frac{\hbar K}{\mu_{PT}}$$

Extension to charge particles

$$\chi(b) = \underbrace{\chi_N(b)}_{\text{Nuclear}} + \underbrace{\chi_C(b)}_{\text{Coulomb}}$$

Corrected to overcome divergences due to the Coulomb potential.

Elastic cross sections for n+^{40}Ca at different incident energies

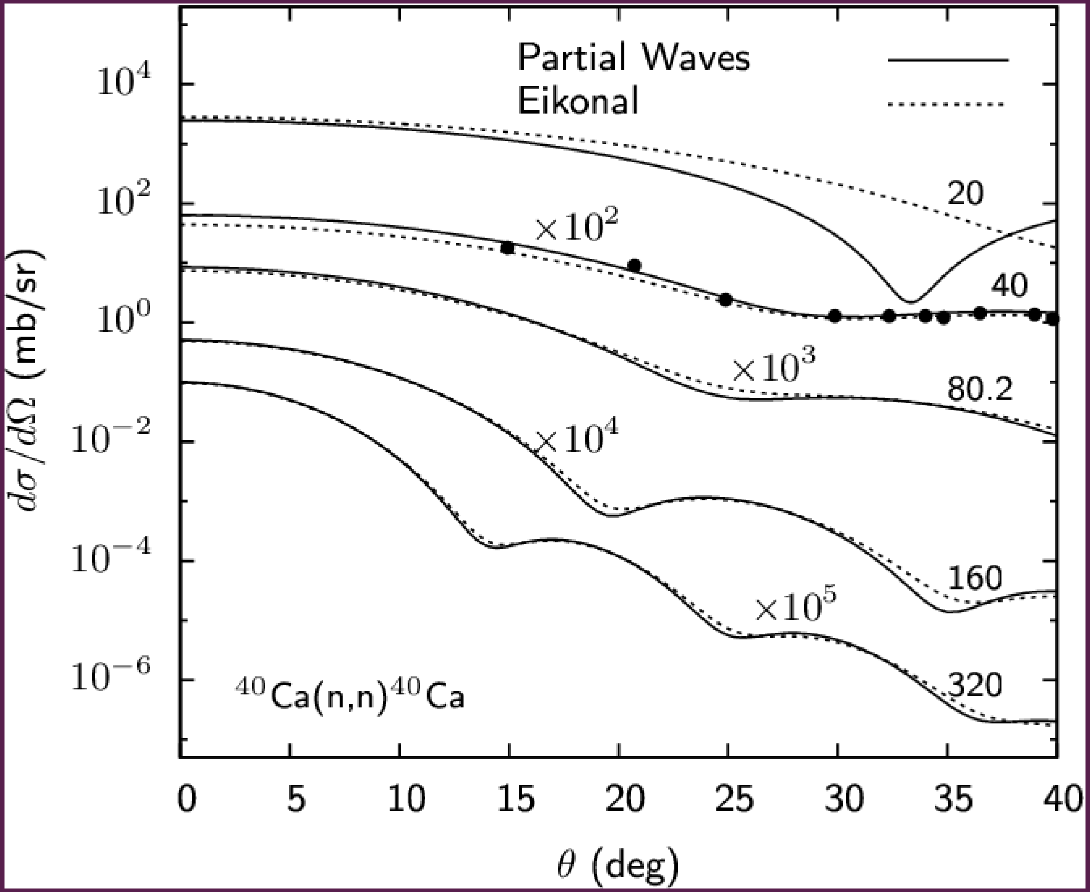

Fig 1. The energies are shown in MeV. The n+^{40}Ca potential is taken from *A. J. Kooning and J. P. Delaroche,* Nucl. Phys. A 713, 231 (2003).

❖ Excellent agreement between both methods when the energy increases.

Elastic cross sections for p+^{40}Ca at different incident energies

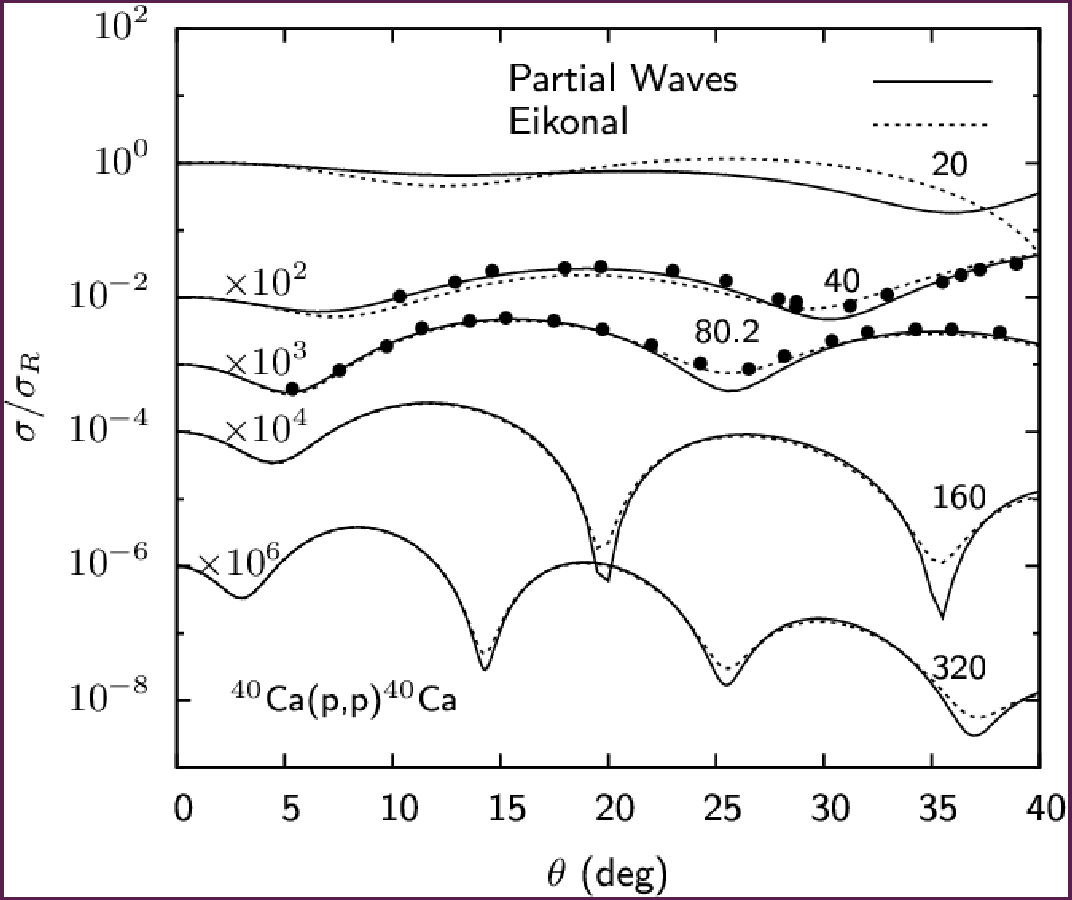

Fig 2. The energies are shown in MeV. The p+^{40}Ca potential is taken from *A. J. Kooning and J. P. Delaroche,* Nucl. Phys. A 713, 231 (2003).

❖ Excellent agreement between both methods when the energy increases.

Four-body eikonal

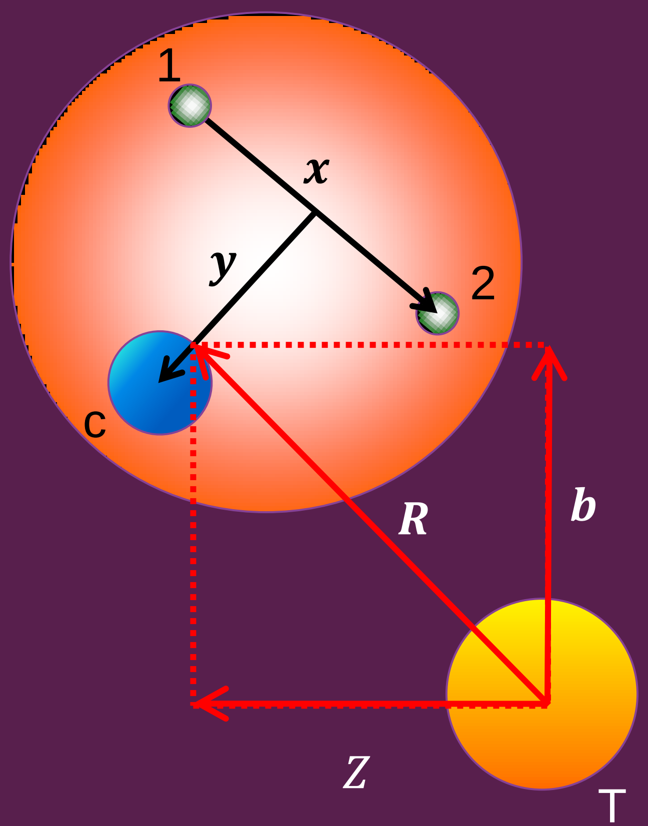

$$H_{4B}\Phi = \mathrm{E_T}\Phi, \qquad E_T = E_0 + \frac{\hbar^2 K^2}{2\mu_{PT}}$$

$$H_{4B} = -\frac{\hbar^2}{2\mu_{PT}}\nabla_R^2 + V_{PT} + H_{3B},$$

$E_0 \rightarrow$ G. S. energy of the projectile

$\frac{\hbar^2 K^2}{2\mu_{PT}} \rightarrow$ Initial relative P.T. energy

Nuclear optical potentials + Coulomb

$$V_{PT} = V_{cT} + V_{Tn} + V_{Tn}$$

Factorizing: $\Phi(\boldsymbol{R},\boldsymbol{x},\boldsymbol{y}) = e^{iKZ}\hat{\phi}(\boldsymbol{R},\boldsymbol{x},\boldsymbol{y})$

$$\rightarrow \left(-\frac{\hbar^2}{2\mu_{PT}}\nabla_{\mathrm{R}}^2 - i\hbar\partial_Z + V_{PT}\right)\hat{\phi} = 0$$

The eikonal approx.
(High-energies)

$$|\nabla^2\hat{\phi}| \ll K|\partial_Z\hat{\phi}|$$

Four-body eikonal

Eikonal w. f. $\longrightarrow$ $\widehat{\Phi}^{\text{eik}}(\boldsymbol{R},\boldsymbol{x},\boldsymbol{y}) \approx \Psi_0(\boldsymbol{x},\boldsymbol{y})\exp\left[-\frac{i}{\hbar v}\int_{-\infty}^{Z} V_{PT}(\boldsymbol{b},\boldsymbol{Z}',\boldsymbol{x},\boldsymbol{y})dZ'\right]$

Eikonal elastic amplitude $\longrightarrow$ $S(\boldsymbol{b}) = \left\langle \underbrace{\Psi^{J_0 M_0{}' \pi_0}}_{\text{3B bound state}} \middle| e^{i\chi(\boldsymbol{b})} \middle| \underbrace{\Psi^{J_0 M_0 \pi_0}}_{\text{3B bound state}} \right\rangle$ $\longrightarrow$ $f(\theta)$

Eikonal breakup amplitude $\longrightarrow$ $S(\boldsymbol{b}) \propto \left\langle \underbrace{\Psi_{k_x K_y}(E)}_{\text{3B scattering State R-matrix}} \middle| e^{i\chi(\boldsymbol{b})} \middle| \underbrace{\Psi^{J_0 M_0 \pi_0}}_{\text{3B bound state}} \right\rangle$ $\longrightarrow$ Bup obs.

Eikonal phase
(Dynamics information) $\longrightarrow$ $\chi(\boldsymbol{b}) = -\frac{i}{\hbar v}\int_{-\infty}^{\infty}[V_{CT}(\boldsymbol{b}) + V_{nT}(\boldsymbol{b}) + V_{nT}(\boldsymbol{b})]\text{dZ}$

Three-body projectile

Three-body model of the projectile

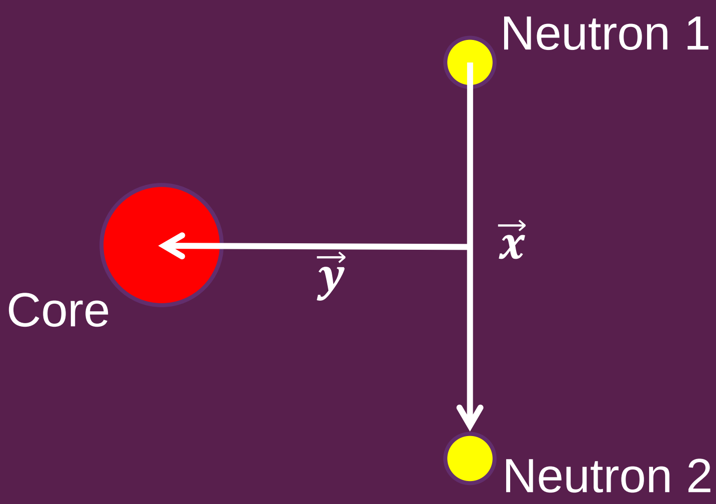

$\vec{x}, \vec{y}$: Jacobi coordinates

ρ,α: Hyperspherical coordinates

$\rho^2 = x^2 + y^2$: Hyperradius

$\alpha = \arctan\left(\frac{y}{x}\right)$: Hyperangle

$\Omega_5 = (\alpha, \Omega_x, \Omega_y)$

$$H_{3B}\Psi^{J\pi} = E\Psi^{J\pi}$$

$E < 0 \rightarrow$ Bound state

$E > 0 \rightarrow$ Scattering states

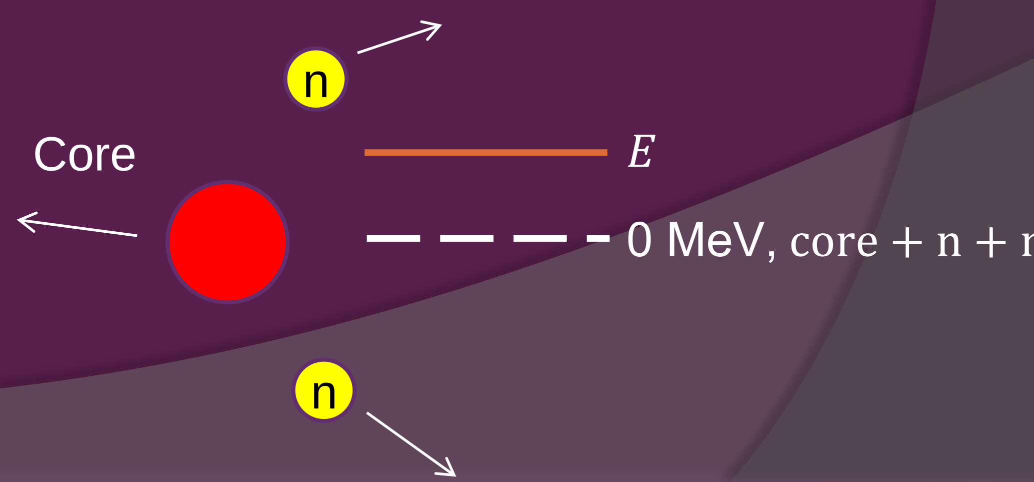

Three-body model of the projectile

$$H_{3B}\Psi^{J\pi} = E\Psi^{J\pi}$$

$$H_{3B} = -\frac{\hbar^2}{2m_n}\nabla_x^2 - \frac{\hbar^2}{2m_n}\nabla_y^2 + T_{c.m.} + \sum_{i<j} V_{ij}$$

2B potentials, Vcn Gaussian, W. Saxon

Kmax

$$\Psi^{J\pi} = \rho^{-5/2}\sum_{K=0}^{\infty}\sum_{\gamma}\chi_{\gamma K}^{J\pi}(\rho)\mathcal{Y}_{\gamma K}^{JM}(\Omega_5)$$

Hyperradial Function (Unknown)

Eigenfunction of angular momentum *K* (Known)

$\pi = (-1)^K \rightarrow$ Parity of the relative motion of the 3B

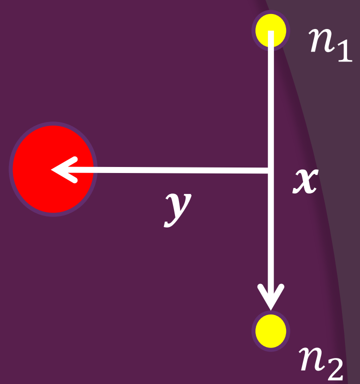

$$\gamma = (l_x, l_y, L, S)$$

$$\hat{L} = \hat{l}_x + \hat{l}_y$$

$$\hat{S} = \hat{S}_1 + \hat{S}_2$$

$$\hat{J} = \hat{L} + \hat{S}$$

Three-body bound states

$$H_{3B}\Psi^{J\pi} = E\Psi^{J\pi}$$

$$\Psi^{J\pi} = \rho^{-5/2}\sum_{K=0}^{\infty}\sum_{\gamma}\chi_{\gamma K}^{J\pi}(\rho)\mathcal{Y}_{\gamma K}^{JM}(\Omega_5)$$

$$\chi_{\gamma K}^{J\pi}(\rho) = \sum_{i=1}^{N} C_{\gamma K i}^{J\pi}\, u_i(\rho),$$

Eigenvalue problem

Lagrange basis

It facilitates the calculations

Three-body continuum states

We employ three different methods to calculate continuum states:

R-matrix

- Precise treatment.
- It calculates three-body continuum states with the correct asymptotic behavior.
- Time consuming calculations.

Pseudostates and Complex scaling

- Approximate methods.
- Discretized the continuum.
- Easy to implement.

Three-body continuum states: R-matrix

Internal region

$$\chi_{\gamma K}^{J\pi}(\rho) = \sum_{i=1}^{N} C_{\gamma K i}^{J\pi} u_i(\rho)$$

External region

$$\chi_{\gamma K}^{J\pi}(\rho \to \infty)$$

a ρ

Nuclear + Coulomb + Centrifugal potentials

Coulomb + Centrifugal potentials

$$\chi_{\gamma K}^{J\pi}(\rho \to \infty) = A_{\gamma K}^{J\pi}\left[H_{\gamma K}^{-}(k\rho)\delta_{\gamma\gamma'}\delta_{KK'} - U_{\gamma K,\gamma' K'}^{J\pi} H_{\gamma K}^{+}(k\rho)\right]$$

Hankel functions

$U_{\gamma K,\gamma' K'}^{J\pi}$ → Collision matrix → $e^{2i\delta}$ → Eigenphases

→ Large matrix for typical γK values

Dimension of the R-matrix calculations

$J=0^+$		$J=1^-$		$J=2^+$	
Kmax	**γK**	**Kmax**	**γK**	**Kmax**	**γK**
12	28	9	40	12	99
16	45	13	77	16	172
20	66	17	126	20	265

$$\gamma = (l_x, l_y, L, S)$$

$N \rightarrow$ Number of Lagrange basis, typical $N = 40$

$\gamma K \rightarrow$ Channels number

Matrices of $\rightarrow \gamma K N \times \gamma K N$

Example: $J = 2^+$ and $K\max = 20$

Matrices of $\rightarrow \gamma K N \times \gamma K N = 265 \cdot 40 \times 265 \cdot 40 = \underline{10600} \times \underline{10600}$

Three-body Continuum states: Pseudostates

Expanded in a completed basis

$$\chi_{\gamma K}^{J\pi}(\rho) = \sum_{i=1}^{N} C_{\gamma K i}^{J\pi} u_i(\rho)$$

Eigenvalue problem

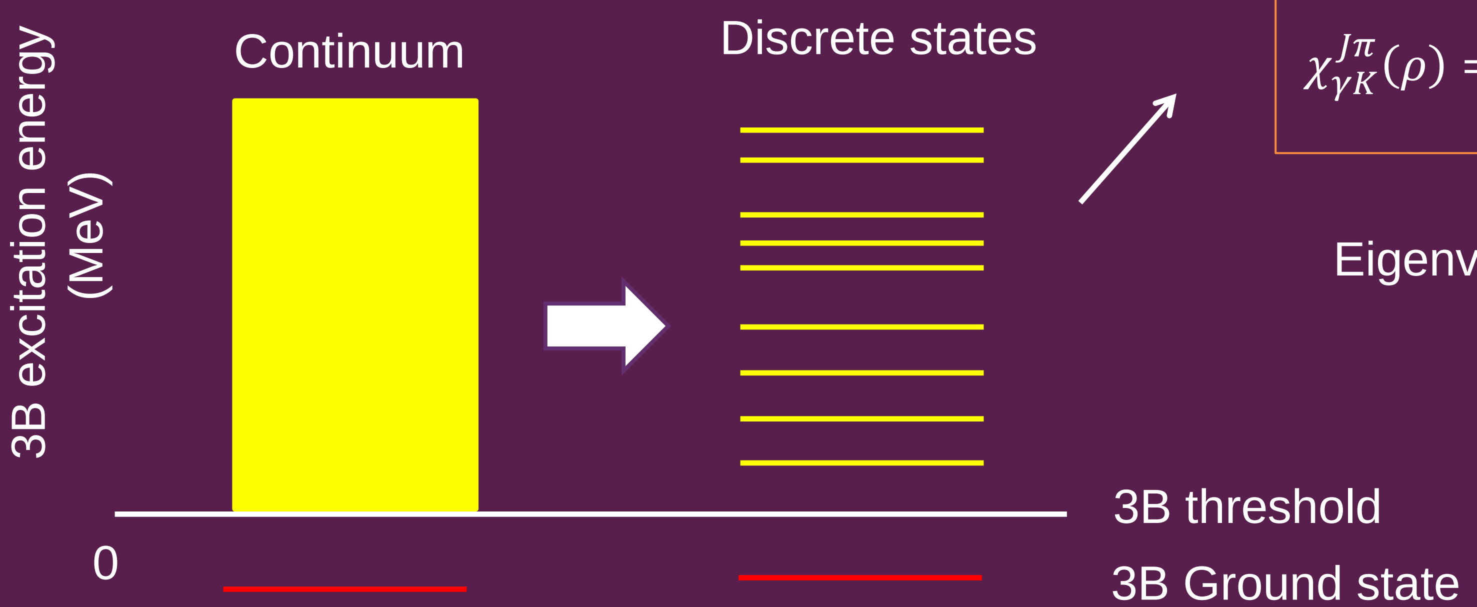

- Bound state variational calculations extended to positive energies:
- It depends on the choice of the basis.

Three-body continuum states: Complex scaling

In complex scaling:

We change $$\boxed{\rho \to \rho e^{i\theta}, \quad k \to k e^{-i\theta}}$$

And solve $$H_{3B}(\theta)\Psi^{J\pi} = E\Psi^{J\pi}$$

with $$\Psi^{J\pi} = \rho^{-5/2} \sum_{K=0}^{\infty} \sum_{\gamma} \chi_{\gamma K}^{J\pi}(\rho) \mathcal{Y}_{\gamma K}^{JM}(\Omega_5)$$

By the expansion in a L^2 basis

$$\boxed{\chi_{\gamma K}^{J\pi}(\rho) = \sum_{i=1}^{N} C_{\gamma K i}^{J\pi}(\theta) u_i(\rho)}$$

Applications of the R-matrix method to ^{6}He

Applications for ^{6}He: Three-body resonances

- $R^{J\pi} \longrightarrow U^{J\pi} \longrightarrow (S^{-1}US = e^{2i\delta})$
- Information about three-body resonances is contained in the eigenphases δ.

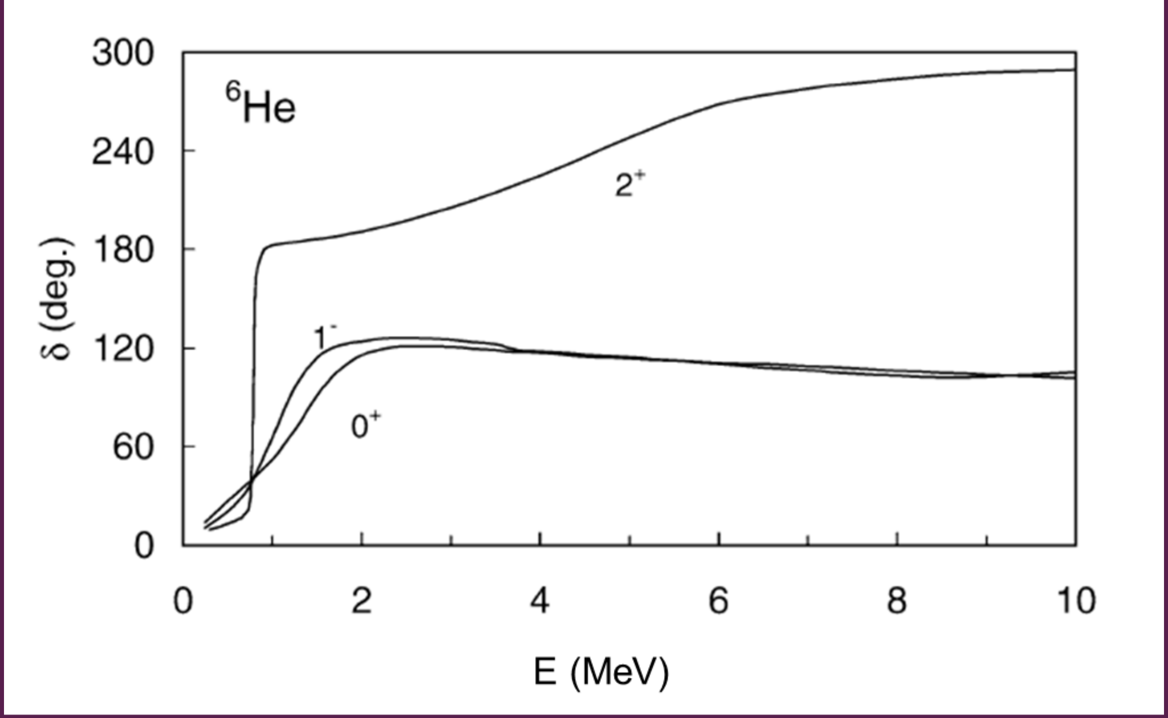

Fig. 3. Eigenphases for ^{6}He for different J values
(From *P. Descouvemont et al, Nucl. Phys. A 765 (2006) 370*).

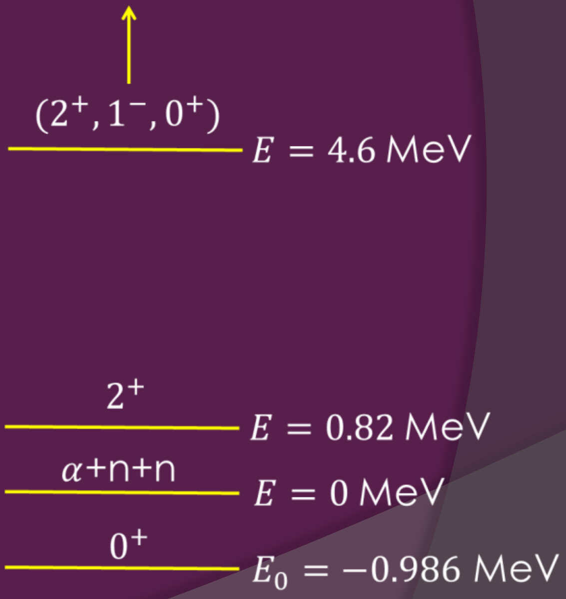

Exp. resonances

Applications for ^{6}He: E1 strength distribution

$$\frac{dB(E_1)}{dE} \propto \left| \underbrace{\left\langle \Psi_{k_x k_y}(E) \right|}_{1^- \text{ 3B cont. R-matrix}} \mathcal{M}^{E1} \underbrace{\left| \Psi^{J_0 M_0 \pi_0} \right\rangle}_{0^+ \text{ 3B bound state}} \right|^2$$

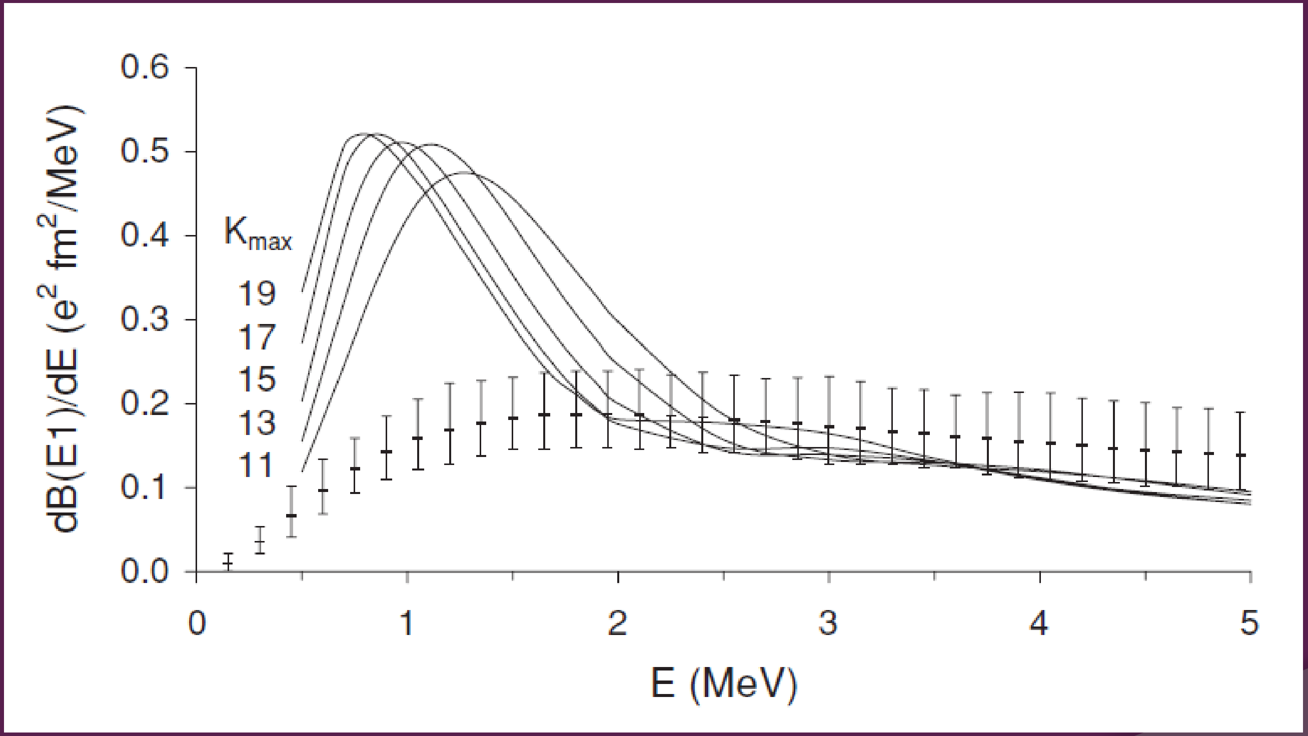

Fig. 4. Electric dipole distribution for different Kmax values. From *D. Baye et al, Phys. ReV. C 79, 024607 (2009)*.

Applications of the pseudostates method to ^6He

Dipole strength of ^{6}He: Continuum pseudostates

$$B_{E1}(E_\lambda) \propto |\underbrace{\langle\psi(E_\lambda)|}_{\text{3B-PS}}\mathcal{M}^{E1}|\underbrace{\Psi^{J_0 M_0 \pi_0}\rangle}_{\text{3B bound state}}|^2$$

Electic dipole transition probability

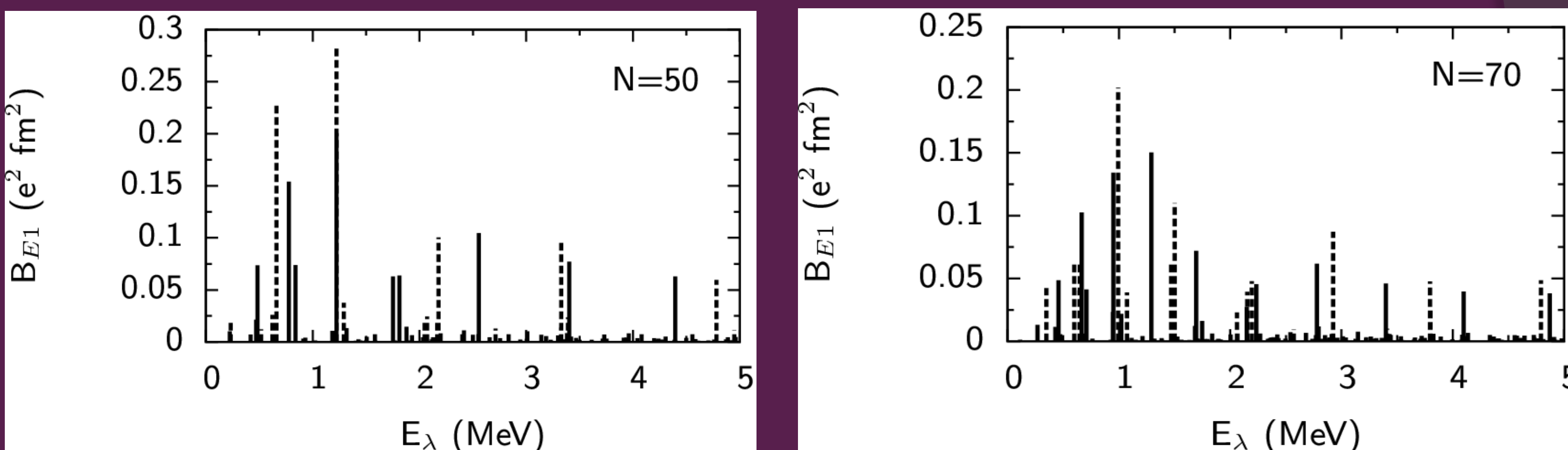

Fig 5. The solid (Lagrange-Laguerre basis) and open bars (Lagrange-Legendre basis) respectively. From *E. C. Pinilla et. al, Nucl. Phys. A 865 (2011) 43.*

Dipole strength distribution of ^{6}He: Pseudostates

$$\frac{dB(E1)}{dE} = \sum_{\lambda} \underbrace{f(E,E_\lambda)}_{\text{Gaussian distribution}} B_{E1}(E_\lambda),$$

$\sigma \rightarrow$ Related with the detector response

Legendre Laguerre

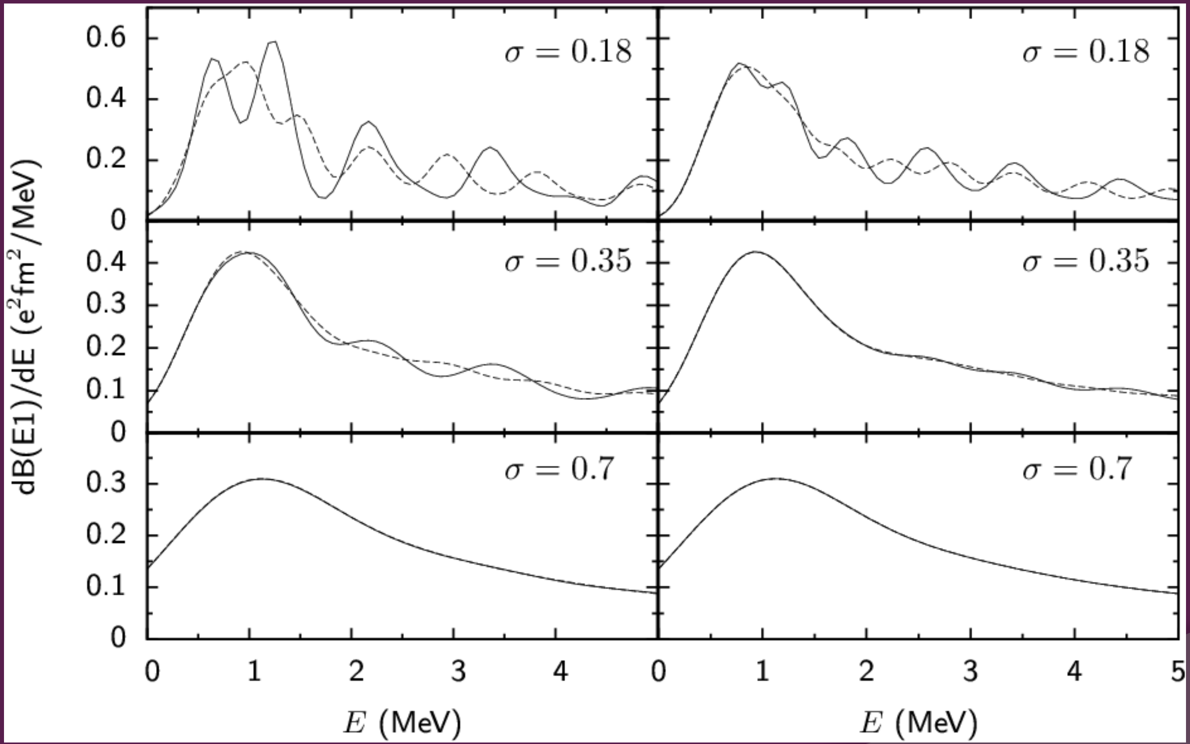

Fig. 6. The solid (dotted) curves are N=50 (N=70) elements of the basis.
From *E. C. Pinilla et. al, Nucl. Phys. A 865 (2011) 43.*

Applications of the complex scaling method to ^{6}He

E1 strength distribution of ^{6}He: Complex scaling

$$\frac{dB^{\theta}(E1)}{dE} = -\frac{1}{\pi}\,\mathrm{Im}\sum_{\lambda}\left(\frac{\left|\langle\widetilde{\Psi}_{\lambda}^{J\pi}(\theta)\|\mathcal{M}_{\theta}^{E1}\|\Psi^{J_0\pi_0}(\theta)\rangle\right|^2}{E - E_{\lambda}^{J}(\theta)}\right)$$

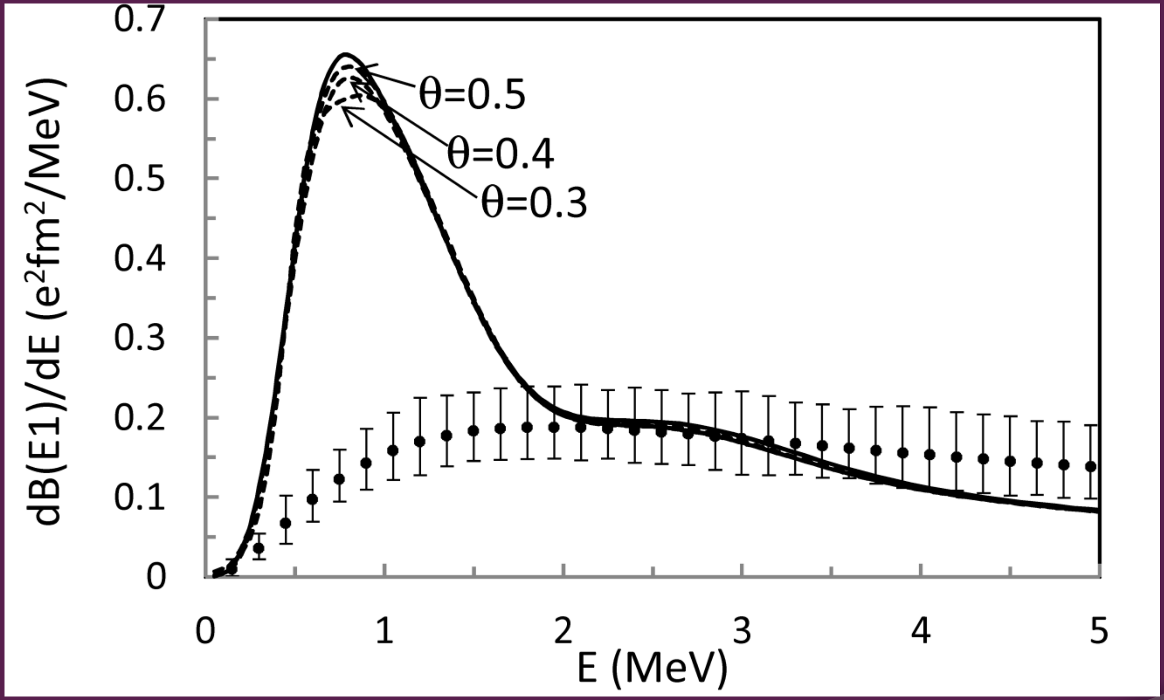

Fig. 7. Complex scaling (dashed curves) and R-matrix (solid curve) dipole strength calculations.

E1 strength distribution of ^{6}He: PS and CS vs. R-matrix

Complex scaling vs. R-matrix

Pseudostates vs. R-matrix

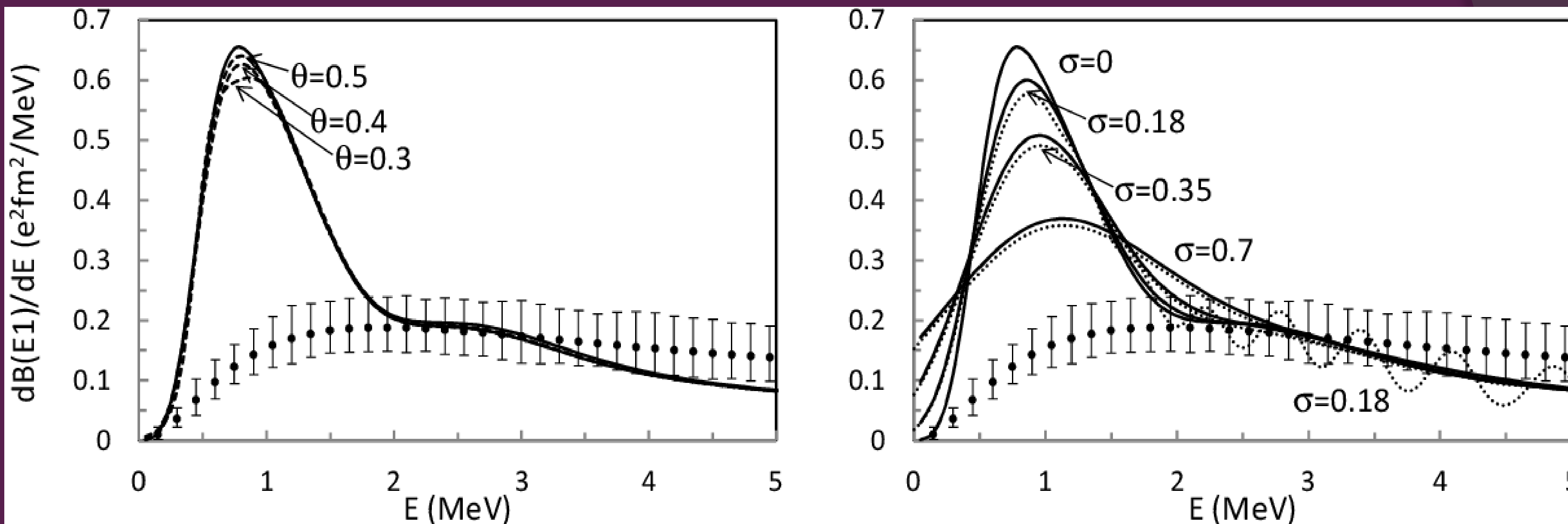

Fig. 8. From *P. Descouvemont, et. al. Proceedings YKIS (2011).* The σ are in MeV and the θ in rad.

Three-body projectile + Target: Four-body eikonal

Four-body eikonal

- Applied by *D. Baye, P. Capel, P. Descouvemont and Y. Suzuki, Phys. ReV. C 71, 024607 (2009).* They described the elastic breakup cross section of ^{6}He on ^{208}Pb @ 70 A MeV.

- **Qualities of the model:**

✓ Contributions different from the dipole.

✓ It does not require ^{6}He-^{208}Pb potential: α-^{208}Pb potential and n-^{208}Pb potential are well known.

✓ It takes nuclear and Coulomb effects and their interference on the same footing.

✓ There is not adjustable parameter.

Applications in ^{11}Li:

E. Pinilla et. al. Phys. Rev. C 85, 054610 (2012)

To calculate bound and scattering states of ^{9}Li+n+n

^{9}Li+n interaction

- From *H. Esbensen, et. al, Phys. ReV. C 56, 3054 (97).*
- Non-existent elastic scattering experimental data.
- Fitted to reproduce a presumed $p_{1/2}$ resonance at 540 keV and a s virtual state.
- ^{9}Li-n interaction multiplied by 1.0056 to reproduce **G.S. energy of ^{11}Li = - 0.378 MeV**.

n+n potential

- Minnesota interaction

We those potentials we well reproduce **r.m.s. radius of ^{11}Li : 3.1 fm** (exp. r.m.s of 3.16 ±0.11 fm).

Eigenphases of ^{11}Li: R-matrix

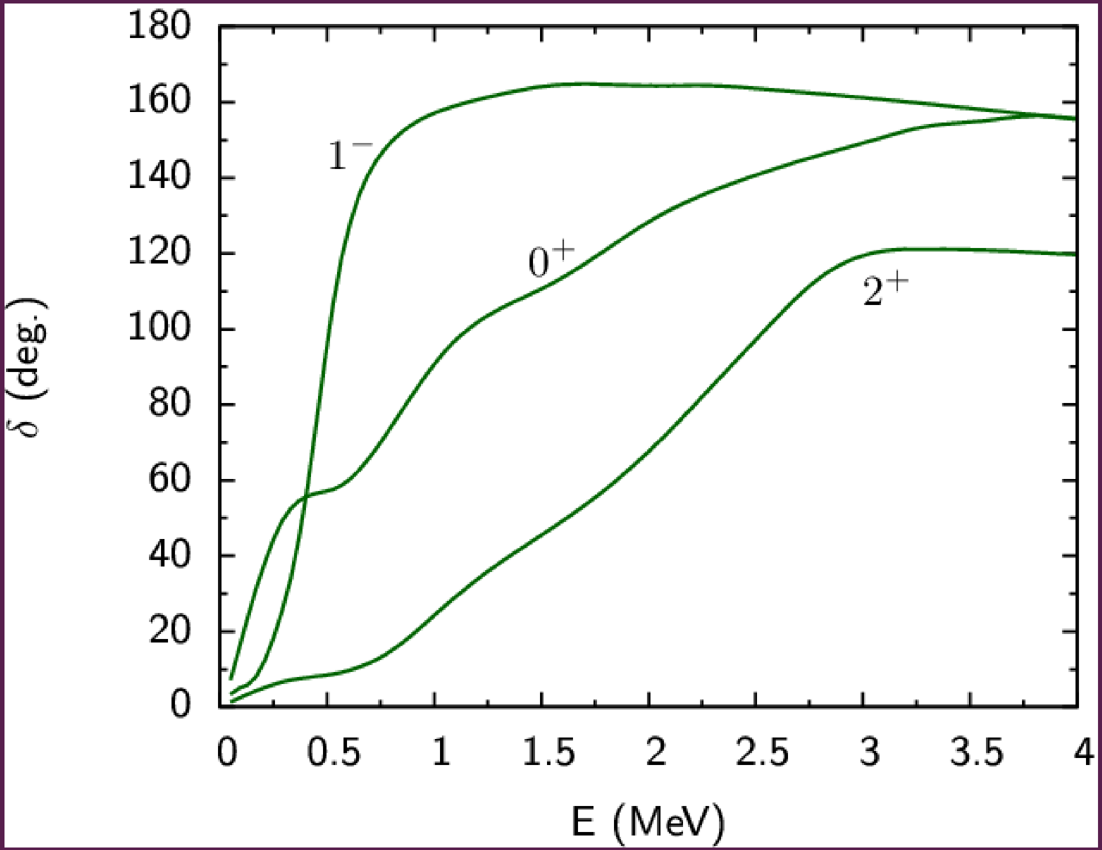

Fig. 9. ^{9}Li+n+n eigenphases

- Like-resonant behavior for 1^- and 2^+ continuum
- Rise of the 0^+ phase shift with energy: "Like a superposition of resonances"

E1 strength distribution of ^{11}Li: PS vs. R-matrix

R-matrix: Solid curves Pseudostates: Dashed curves

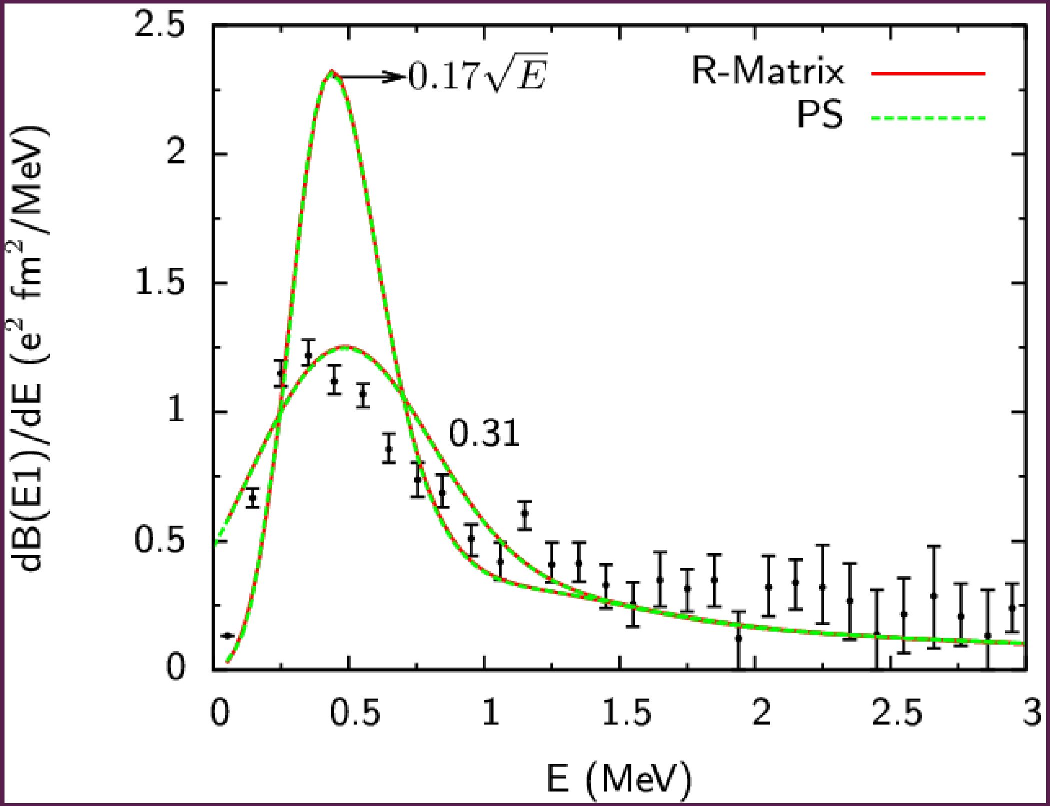

Fig. 10. The values shown are σ in MeV. Experimental Data from *T. Nakamura et. al, Phys. Rev. Lett. 252502 (2006).*

- ❖ Very good agreement between both methods.
- ❖ Our theoretical model overestimate the data.

Conditions of the calculations for ^{11}Li on ^{208}Pb

To calculate the breakup cross sections of ^{11}Li on ^{208}Pb @ 70 A MeV:

❖ **^{9}Li-^{208}Pb potential (lack of the potential):**
Renormalized $(9^{1/3}+208^{1/3})$ α-^{208}Pb interaction @ 70 A MeV of B. Bonin et. al. (Following the same idea of *P. Capel et. al, Phys. Rev. 68, 014612 (2003)* for ^{10}Be on ^{208}Pb).

❖ Variation of the **^{9}Li-^{208}Pb** potential was checked but it did not provide a significant change to the breakup and angular distributions.

❖ **n-^{208}Pb potential**:
Kooning and Delaroche, Nucl. Phys. A 713, 231 (2003).

Breakup cross sections of ^{11}Li on ^{208}Pb @ 70 A MeV

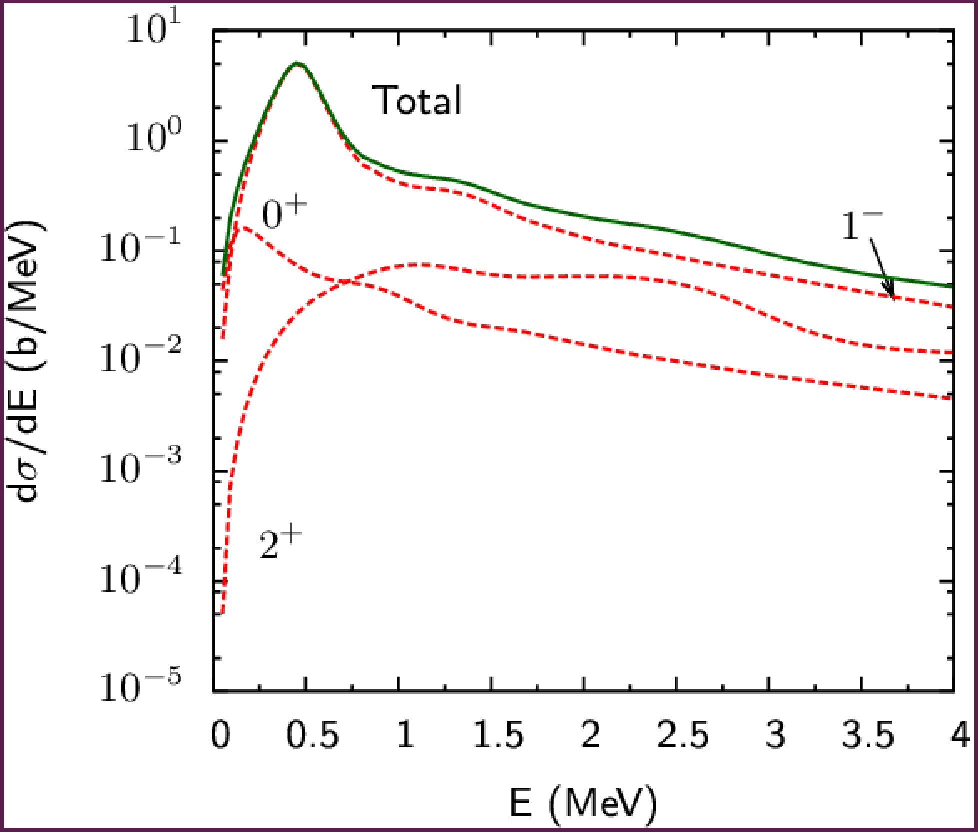

Fig. 11. Partial and total eikonal breakup cross sections.

❖ Small correction of the 0^+ and 2^+ partial waves to the total cross section.

Influence of the core-target potentials on the Partial breakup cross sections

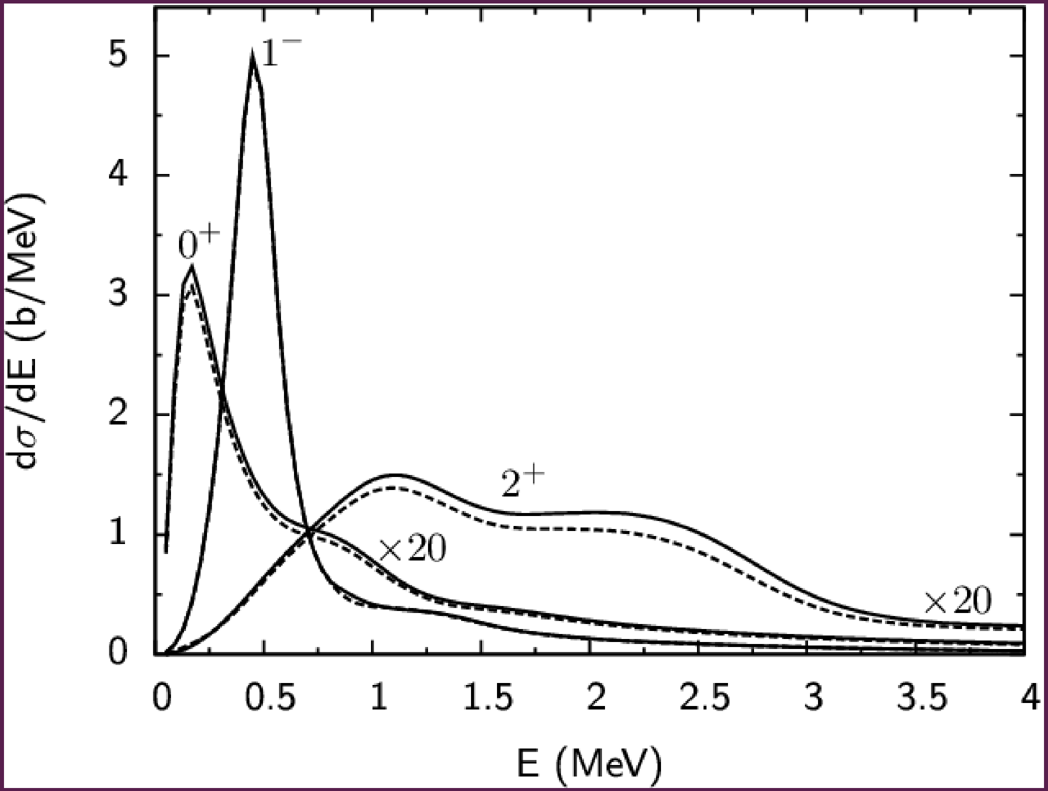

Fig. 12. The solid curves are the original ^{9}Li-potential (renormalized α-^{208}Pb) and the dashed curves are the potential modified by a factor of 2.

❖ Small influence of the choice of the core-target potential.

Convoluted breakup eikonal cross section with the detector response

^{11}Li on ^{208}Pb @ 70 A MeV

Theoretical data convoluted with a Gaussian of $\sigma = 0.17\sqrt{E}$ MeV

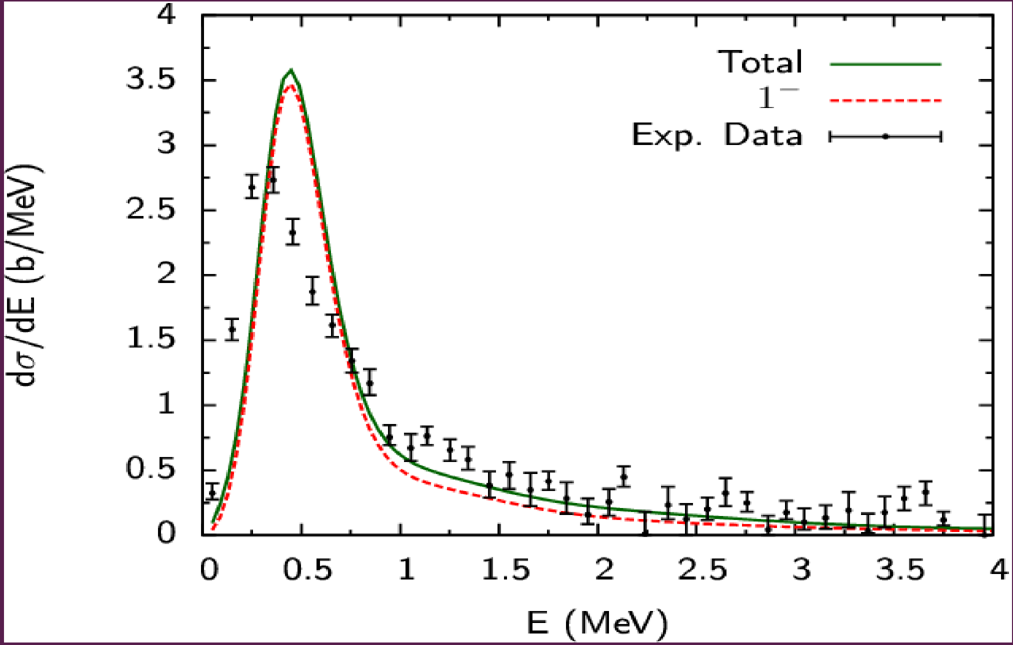

Fig. 13. Exp. Data from *T. Nakamura et. al, phys. Rev. Lett. 252502 (2006).*

❖ Fair agreement with the experimental data.

Angular distributions of ^{11}Li on ^{208}Pb @ 70 A MeV

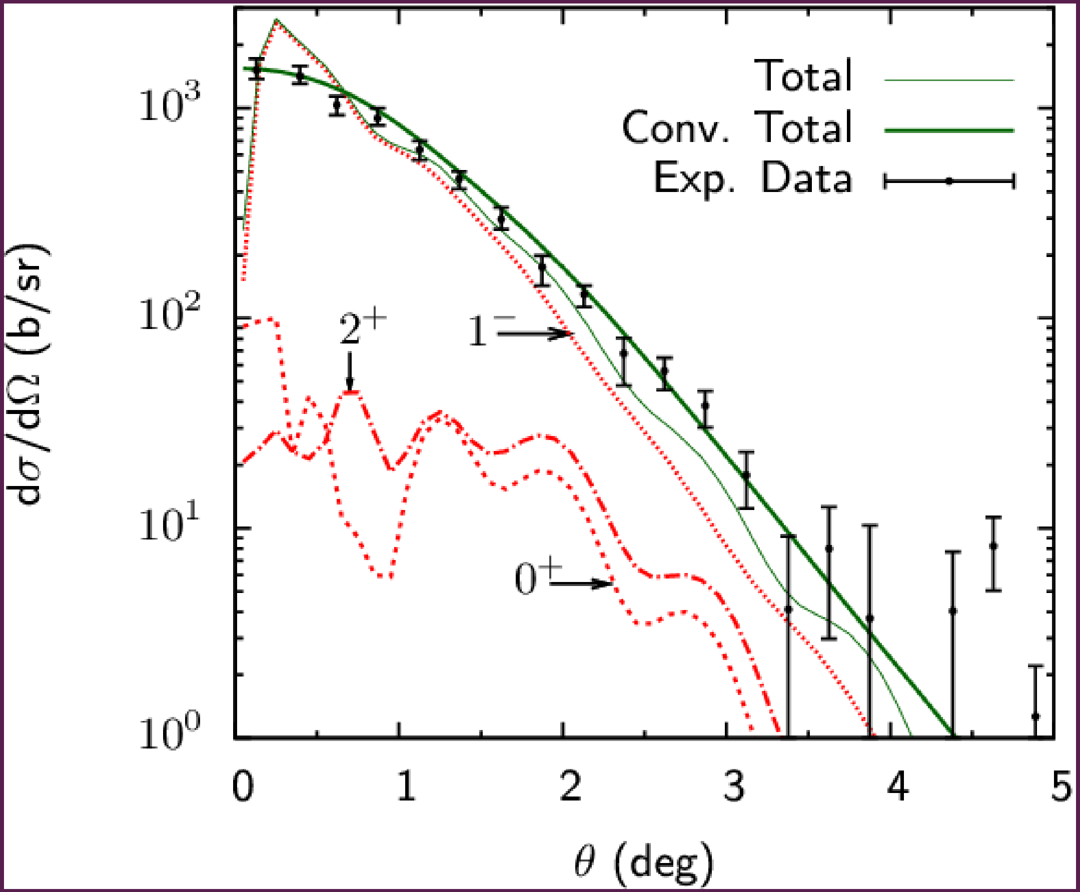

Fig. 14. Partial, total (thin solid) and convoluted total (thick solid) angular distributions. Experimental Data from *T. Nakamura et. al, Phys. Rev. Lett. 252502 (2006).*

- Very good agreement of the total convoluted curve for almost all angles.

Convoluted E1 strength distribution of ^{11}Li with the detector response

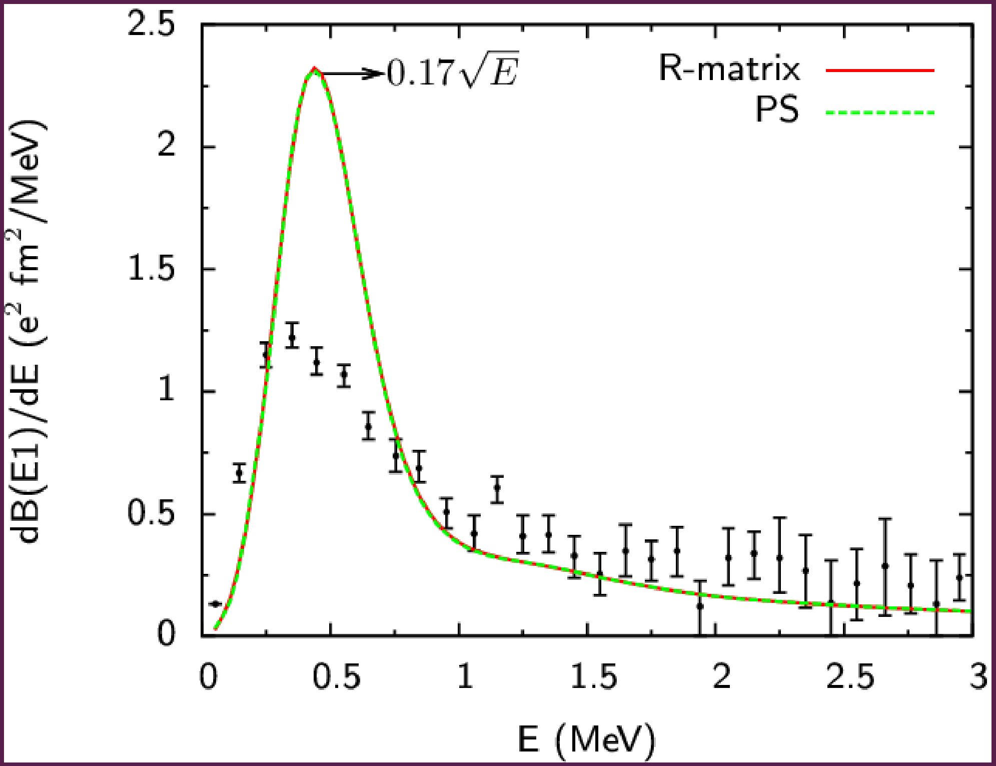

Fig. 15. The σ value is in MeV. Experimental Data from *T. Nakamura et. al, Phys. Rev. Lett. 252502 (2006).*

❖ **Why we overestimate the E1 distribution?**

Why we overestimate the E1 distribution?

In the breakup reactions of $^{11}Li+^{208}Pb$ @ 70 A MeV

- $\frac{d\sigma}{dE}$ is measured directly $\longrightarrow$ We fit the data
- $\frac{d\sigma}{d\theta}$ is measured directly $\longrightarrow$ We fit the data
- $\frac{dB(E1)}{dE}$ is measured indirectly $\longrightarrow$ We do not fit the data

(It depends on model assumptions)

How is determined experimentally dB(E1)/dE?

It is extracted from the equivalent photon method as

$$\frac{d\sigma^{\text{Exp}}}{dE} = \frac{16\pi^3}{9\hbar c}\frac{dB^{\text{Exp}}(E1)}{dE}\int_{b_{min}}^{\infty} 2\pi db b\, N_{E1}(b,E)$$

❖ $N_{E1}(b,E) \rightarrow$ Number of virtual photons incident on ^{11}Li by unit area.

❖ $\frac{dB^{\text{Exp}}(E1)}{dE} \rightarrow$ Structure information of ^{11}Li.

❖ It comes from semi-classical perturbation theory.

❖ It is assumed to be one step and dominated by a single E1 multipolar transition.

❖ From b_{min} to exclude nuclear excitation.

^{11}Li is excited by absortion of a virtual photon from the Coulomb field of the target.

Estimation of the b_{min} dependence in the dipole distribution of ^{11}Li

In non-relativistic regime

$$\boxed{\frac{dB^{\mathrm{Exp}}(E1)}{dE} = \frac{9}{32\pi}\left(\frac{\hbar v}{Z_T e}\right)^2 \frac{1}{\xi_{min}K_0(\xi_{min})K_1(\xi_{min})}\frac{d\sigma^{\mathrm{Exp}}}{d\Omega}}$$

$v \rightarrow$ Projectile-target relative velocitiy, $\quad \xi_{min} = \frac{E-E_0}{\hbar v} b_{min},$

$E \rightarrow$ Excitation energy of ^{11}Li, $\quad E_0 \rightarrow$ G. S. energy of ^{11}Li

$b_{min} = \frac{Z_P Z_T e^2}{2\,\mathrm{E_{PT}}\tan\left(\frac{\theta_c}{2}\right)} \rightarrow$ Min. Impact parameter for the semi-classical Coulomb trajectory

$\theta_c \rightarrow$ maximum scattering angle (beyond θ_c nuclear interaction is important)

Estimation of the θ_c dependence in the dipole distribution of ^{11}Li

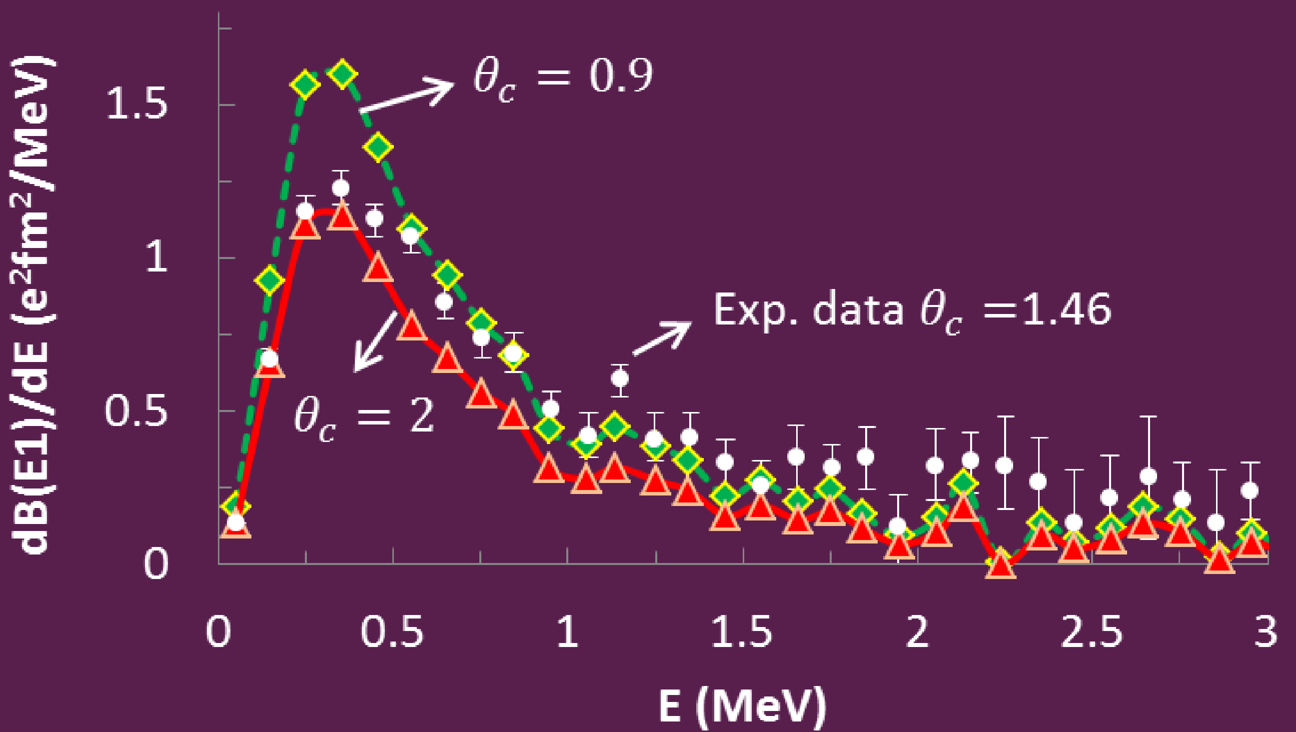

Fig. 16. The θ_c values of 0.9, 1.46 and 2 deg correspond to b_{min} of 31, 19 and 14 fm respectively.

- Small θ_c provides a larger dipole distribution at low excitation energies.

Elastic scattering of ^{11}Li on ^{208}Pb @ 70 A MeV in the Eikonal method

Original ^{9}Li-target (Red curves)

^{9}Li-target X 2 (Green curves)

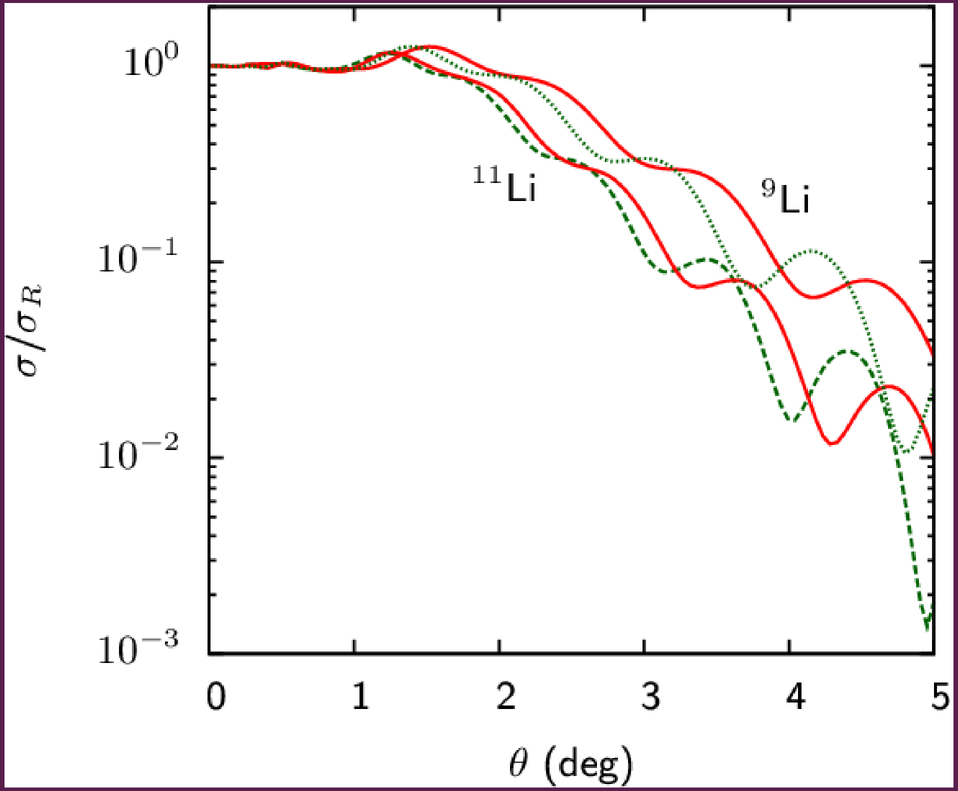

- Reduction in the ^{11}Li+^{208}Pb elastic scattering due to flux going to breakup
- $0 \lesssim \theta \lesssim 1 \rightarrow$ Rutherford scattering.
- Influence of the choice of the core-taget potential.

Angular distributions of ^{11}Li on ^{208}Pb @ 70 A MeV

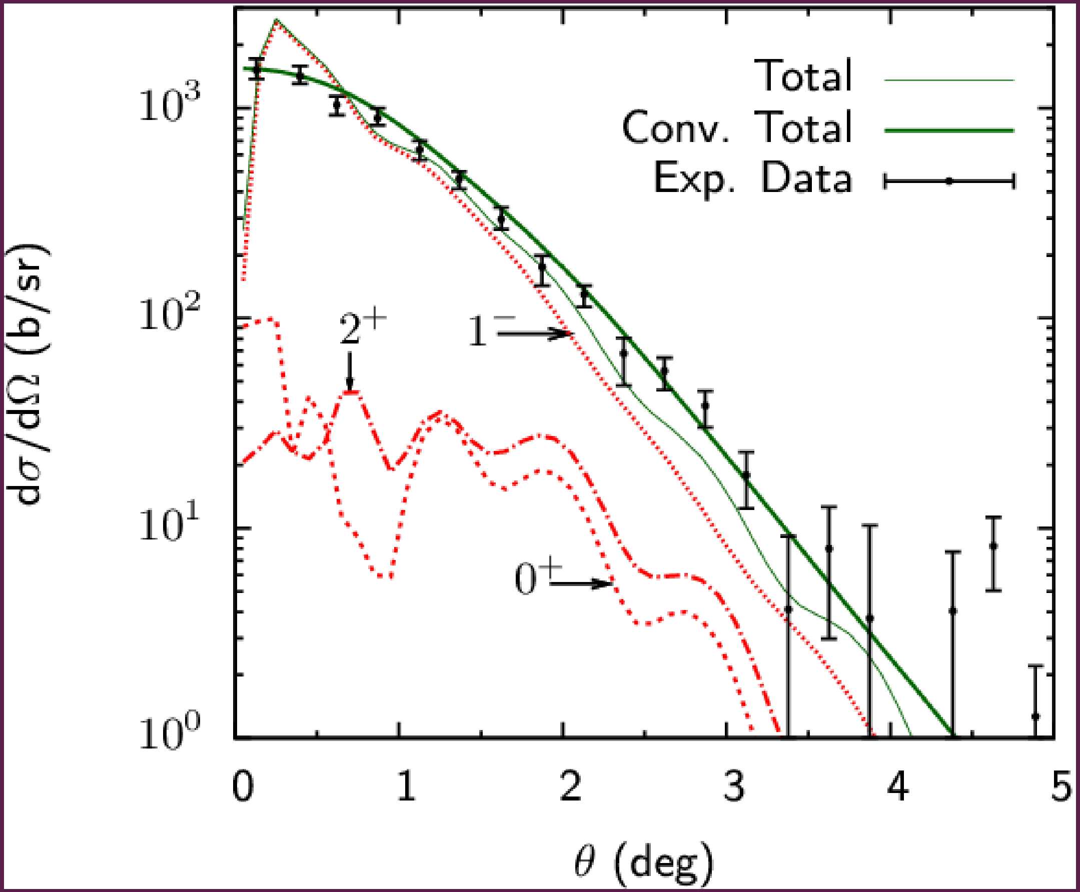

Fig. 14. Partial, total (thin solid) and convoluted total (thick solid) angular distributions. Experimental Data from *T. Nakamura et. al, Phys. Rev. Lett. 252502 (2006).*

- Very good agreement of the total convoluted curve for almost all angles.

Conclusions

❖ We confirmed the existence of a dipole resonance.

❖ The breakup cross sections and angular distributions of ^{11}Li on ^{208}Pb are in good agreement with the experimental data.

❖ We suggest that the simple Coulomb dipole approximation, traditionally used to extract experimental dipole strengths, should be replaced by more elaborate models.

❖ A standard problem in few body cluster calculations is that we do not have optical potentials for core-target interactions. It will be great! If more experiments on elastic scattering were done.

❖ Elastic scattering experiments at the same energy of ^{11}Li on ^{208}Pb will be very useful to evaluate the precision of the present eikonal model.

Thank you for your attention